

A high-order arbitrarily unstructured finite-volume model of the global atmosphere: tests solving the shallow-water equations

Hilary Weller^{1,*} Henry G. Weller²

¹ Walker Institute, Meteorology Department, University of Reading, UK

² OpenCFD Ltd, www.opencfd.co.uk

SUMMARY

Simulations of the global atmosphere for weather and climate forecasting require fast and accurate solutions and so operational models use high-order finite differences on regular structured grids. This precludes the use of local refinement; techniques allowing local refinement are either expensive (eg. high-order finite element techniques) or have reduced accuracy at changes in resolution (eg. unstructured finite-volume with linear differencing).

We present solutions of the shallow-water equations for westerly flow over a mid-latitude mountain from a finite-volume model written using OpenFOAM. A second/third-order accurate differencing scheme is applied on arbitrarily unstructured meshes made up of various shapes and refinement patterns. The results are as accurate as equivalent resolution spectral methods. Using lower order differencing reduces accuracy at a refinement pattern which allows errors from refinement of the mountain to accumulate and reduces the global accuracy over a 15 day simulation. We have therefore introduced a scheme which fits a 2D cubic polynomial approximately on a stencil around each cell. Using this scheme means that refinement of the mountain improves the accuracy after a 15 day simulation.

This is a more severe test of local mesh refinement for global simulations than has been presented but a realistic test if these techniques are to be used operationally. These efficient, high-order schemes may make it possible for local mesh refinement to be used by weather and climate forecast models.

Copyright © 2000 John Wiley & Sons, Ltd.

KEY WORDS: Adaptive, differencing, atmosphere, shallow water, unstructured, finite volume

1. Introduction

Adaptive and variable resolution modelling of the atmosphere is an expanding area of research due to the potential benefits to, for example, regional climate and weather forecasting and cyclone tracking eg. [3, 11, 4, 2, 7, 10]. There are however still challenges before these techniques can compete in accuracy and efficiency with techniques used for fully structured, uniform grids.

There are a number of ways of achieving variable resolution: Berger and Olinger [3] used nesting of finer structured grids within coarser grids, Bacon et. al. [2] use a Delaunay triangulation of two-dimensional space and Iske and Kaser [6] use a Voronoi decomposition of space. Alternatively, one can deform a structured mesh [12] or refinement patterns must persist all around the globe [13]. We have implemented the shallow-water equations in OpenFOAM (www.opencfd.co.uk) which can handle any mesh structure. This allows us to test the accuracy of different mesh structures.

*Correspondence to: h.weller@rdg.ac.uk

Contract/grant sponsor: NERC, National Centre for Atmospheric Science, Climate

Finite-volume models are appropriate for atmospheric modelling due to their inherent conservation, availability of bounded differencing schemes [15], applicability to any mesh structure [6] and availability of efficient, segregated implicit solution algorithms [5]. Cell-centre/face-centre staggered finite-volume algorithms usually use linear differencing however, which is only first-order accurate where the mesh is non-uniform [1] and which we will show is not sufficient for global atmospheric models. We will present results using a second/third-order differencing scheme that maintains this accuracy regardless of mesh uniformity or regularity.

The shallow-water equations describe much of the atmosphere's behaviour in the horizontal, allowing tests of discretisation. Results are presented of the Williamson [17] test case with westerly flow over a mid-latitude mountain. This test case enables examination of the effect of local mesh refinement on global errors. Low resolution can result in poor representation of orography and, in the real atmosphere, orographic impacts on the flow can be due to small-scale diabatic processes such as orographic rainfall. There are numerical difficulties due to the changes in accuracy where the mesh becomes finer however; grid-scale waves travelling from the fine mesh to the coarse mesh could be refracted or reflected. The change in accuracy could alter the geostrophic balance which will be a source of unbalanced waves. These problems will be severe in this adiabatic, frictionless test case. A more complete model of the atmosphere will suffer from the same errors where the mesh changes resolution but should also benefit from more accurate representation of diabatic terms.

The model, including the new differencing scheme and the meshes used, is described in section 2, results are presented in section 3 and final conclusions drawn in section 4.

2. Model Description

2.1. *Williamson et al. Test Case [17]*

The test case has an isolated, mid-latitude mountain and initial conditions consisting of shear free westerly flow in geostrophic balance with the geopotential height. As the flow hits the mountain, the balance between the Coriolis force and pressure gradient is reduced, generating gravity and Rossby waves. After 15 days these Rossby waves have spread around both hemispheres. A reference solution calculated from a very high resolution spectral model is available from <ftp.ucar.edu/champp/shallow>.

2.2. *OpenFOAM*

OpenFOAM is a public domain, open source computational fluid dynamics toolkit developed and released by OpenCFD (www.opencfd.co.uk) using the finite-volume technique on three-dimensional arbitrarily unstructured meshes. (This means that the cells can be any 3D shape.) Some of the coding practices are described by [16] and the unstructured finite-volume method by [5].

2.3. *A Shallow-water Equation Solver written using OpenFOAM*

The two-dimensional shallow-water equations in a three-dimensional geometry consist of the momentum and continuity equations:

$$\frac{\partial h\mathbf{U}}{\partial t} + \nabla \cdot h\mathbf{U}\mathbf{U} = -\mathbf{\Omega} \times h\mathbf{U} - gh\nabla(h + h_0), \quad \frac{\partial h}{\partial t} + \nabla \cdot h\mathbf{U} = 0 \quad (1)$$

where \mathbf{U} is the horizontal velocity, ∇ is in the horizontal direction, h is the height of the fluid surface above the solid surface, h_0 is the height of the solid surface above a reference height, $\mathbf{\Omega}$ is the rotation rate of the globe, and g is the scalar acceleration due to gravity.

These equations have been implemented in OpenFOAM on a two-dimensional spherical mesh in Cartesian co-ordinates. The cell-volumes, cell-centres, face-centres and face-areas have been modified for the curved, spherical domain. The prognostic variables are the cell-average momentum, $h\mathbf{U}$, and

height, h , and, to avoid a computational mode, the mass flux between cells (normal to the faces), ϕ . The momentum equation is integrated over each cell and discretised using Gauss' divergence theorem:

$$\frac{\delta V}{\delta t}((h\mathbf{U})^{n+1} - (h\mathbf{U})^n) + \sum(\phi\mathbf{U})_f^{n+\frac{1}{2}} = -\delta V(\boldsymbol{\Omega} \times h\mathbf{U} + gh\nabla_c(h + h_0))^{n+\frac{1}{2}} \quad (2)$$

where δV is the cell-volume, δt is the time step, the superscript represents the time step, \sum means summation over all the faces of a cell, subscript f means interpolation from cell-averages to face averages and ∇_c is the discretised cell-average gradient. This equation is interpolated onto the cell faces and the dot product is taken with the face-area vector, $\delta\mathbf{S}$ (normal to the face with the magnitude of the face-area), to give an equation for the flux, ϕ ($= (h\mathbf{U})_f \cdot \delta\mathbf{S}$):

$$\phi^{n+1} = \frac{1}{A_f}(\phi^n + (H - \delta t \boldsymbol{\Omega} \times h\mathbf{U})_f^{n+\frac{1}{2}} \cdot \delta\mathbf{S} - \delta t gh_f^{n+\frac{1}{2}} \nabla_f^{n+\frac{1}{2}}(h + h_0)) \quad (3)$$

where $H = -\frac{\delta t}{\delta V} \sum \phi \lambda_N \mathbf{U}_N$, $A = 1 + \frac{\delta t}{\delta V} \sum \frac{\phi}{h_f} \lambda$, ∇_f is the discretised gradient at the face dot producted with $\delta\mathbf{S}$ and λ and λ_N are interpolation factors from cell-average values to face average values. Equation 3 is substituted into the continuity equation to obtain an equation for the height:

$$\frac{\delta V}{\delta t}(h^{n+1} - h^n) + \sum \phi^{n+\frac{1}{2}} = 0 \quad (4)$$

The second-order, two time-level Crank-Nicholson scheme is used to solve the discretised momentum and height equations implicitly (separately and with non-linear terms lagged) and the flux equation explicitly. The lagged new time level values are updated and all equations are solved once again at each time step. This solution procedure is described in more detail by [5]. The old time-level flux is interpolated from the old time-level momentum so that they remain consistent. This separation by one time step between the momentum and the flux is enough so that no computational mode is excited in this slowly evolving case where all features are well resolved. For cases in which grid scale gravity waves are excited, the old time-level flux is blended with the old momentum so that they remain consistent while removing the computational mode. The details of this blending is the subject of current research. It remains to define how the interpolations from cell-averages to faces and gradients are estimated.

2.4. Interpolations and Gradients

To make discretisation on arbitrarily unstructured meshes simple, cell-volume average quantities are approximated by the cell-centre value and face-area averages are approximated by face-centre values. These approximations are second-order accurate but we have still found advantage from using higher-order schemes to interpolate from cell-centre values to face-centres and for estimating gradients.

2.4.1. The quasi-cubic differencing scheme A simple way to interpolate onto a face is to use the values and gradients in the two adjacent cells, where the cell-centre gradients are calculated using Gauss' theorem and the face values. This is theoretically only first-order accurate but if the mesh is uniform, polynomials of up to fourth-order can be discretised exactly.

2.4.2. The multidimensional polynomial fit differencing scheme We have implemented a scheme based on [9] that fits a polynomial around each cell for interpolates and gradients. A two-dimensional cubic polynomial is fit for the neighbourhood of each cell using a local co-ordinate system. The two-dimensional cubic has 10 unknowns so a stencil of at least 10 cells surrounding each cell is found. As there can be more cells in each stencil than unknowns, a least-squares fit using singular value decomposition is found with the central cells in the stencil weighted so that the fit is most accurate near the centre. The singular value decomposition needs to be done only once per cell at the beginning of the simulation, leaving just n multiplies to calculate an interpolation or a gradient component per

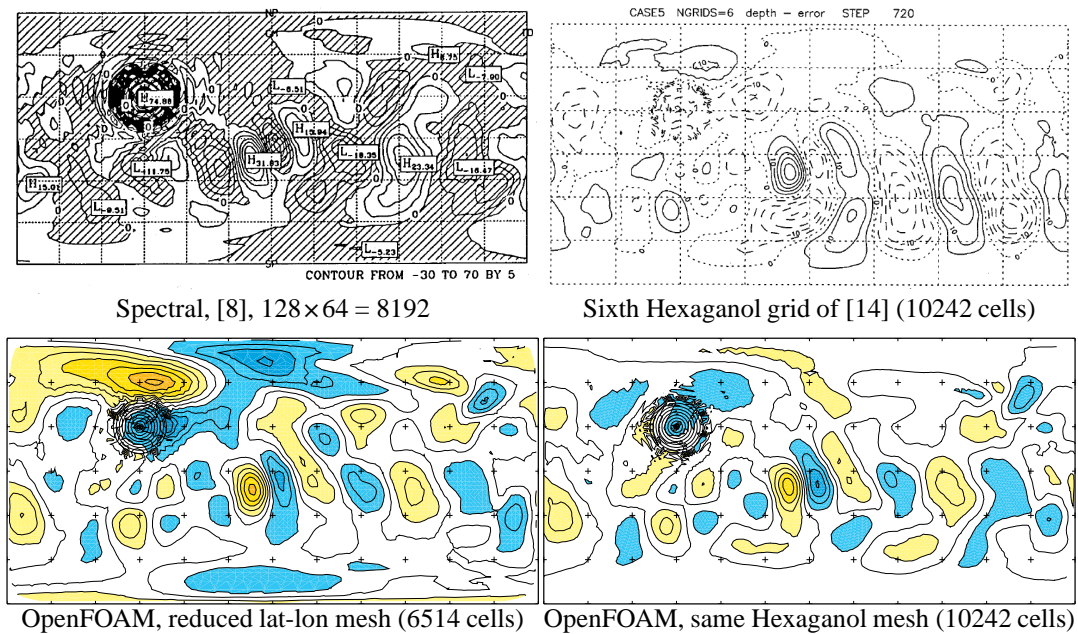


Figure 1. Errors after 15 days for the flow over a mid-latitude mountain. Contour interval is 5m.

time step, where n is the size of the stencil. As this scheme creates a large computational molecule, it is not used to solve equations implicitly as it would create too many inter-cell dependencies and make the linearised equation set expensive to solve. It is therefore used as a deferred correction on linear differencing, as described by [5].

2.5. Model Setup: Meshes and Time Step

Results are presented for three different meshes of the globe; two reduced latitude-longitude meshes, one of which has 2:1 refinement of the mountain and the other a hexagonal-icosohedral mesh as used by Thurn [14]. A time step of 20 minutes is used for consistency with Jacob [8].

3. Results

The method is well-balanced in the presence of orography: the mountain test case was run for 15 days starting from a geostrophically balanced resting state and the maximum speed generated was 0.6cm/s. This was due to inaccuracies in the initial fluid height field not giving an exactly constant total height when added to the mountain height. This initial error persists since total energy is conserved to within 0.05%, vorticity to within $10^{-7}\%$ and enstrophy to within 0.1% over the 15 days.

3.1. Comparisons with previously published results

After 15 days errors in comparison to the reference solution are compared with published errors on grids with similar resolution. Figure 1 shows errors of the spectral model of [8] using 128×64 grid points, the model on a hexagonal-icosohedral mesh of [14] and OpenFOAM results on the reduced latitude-longitude mesh without refinement of the mountain and on the same hexagonal mesh as [14]. All error fields have oscillations around the mountain, especially the spectral model. For the other models, these are due to the oscillations in the spectral reference solution, since discontinuities are not well represented in spectral space.

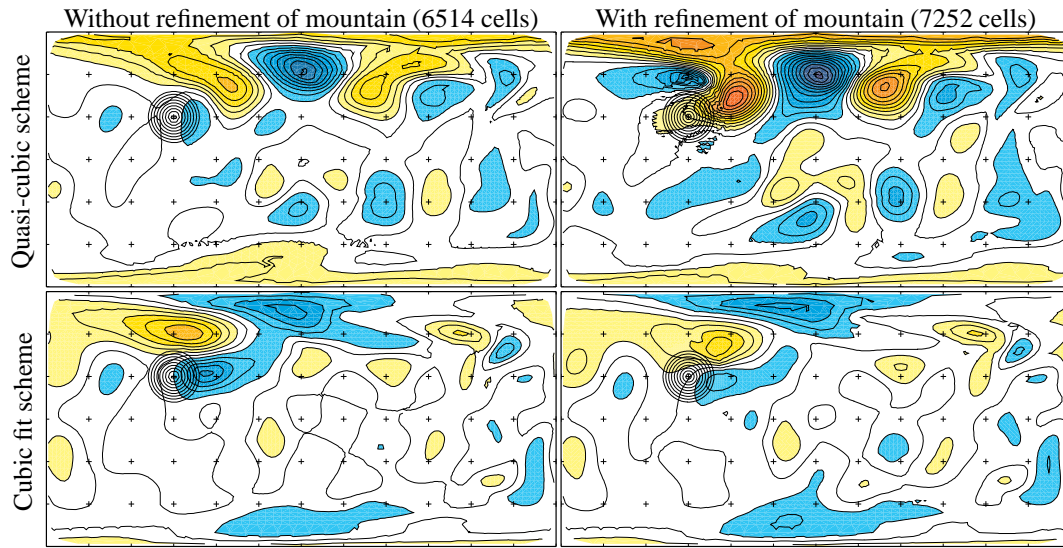


Figure 2. Errors after 15 days for the flow over a mid-latitude mountain on reduced latitude-longitude meshes. Contour interval is 5m.

The OpenFOAM errors on the reduced latitude-longitude mesh are slightly lower than the spectral model in the tropics but larger towards the north pole. This is due to the coarser mesh towards the poles and to errors introduced by the un-refinement patterns themselves. The order of the scheme for estimating values at points has been tested by comparing the discretised gradients of third and fourth-order polynomials with the exact gradients. The cubic fit scheme gives fourth-order accuracy where the mesh is uniform and third-order accuracy at the refinement patterns which could contribute to the larger errors towards the poles.

The OpenFOAM errors on the hexagonal icosohedral mesh are similar but slightly lower than those of [14] on the same mesh. [14] uses quadratic differencing rather than cubic. This test case was also run by [9] and the results improved with higher-order differencing.

3.2. Comparisons between OpenFOAM results

The uniformity of the hexagonal icosohedral mesh reduces the high latitude errors seen for the reduced latitude-longitude mesh (figure 1).

Figure 2 shows results from the latitude-longitude meshes with and without refinement of the mountain and using the quasi-cubic scheme and the new cubic fit scheme. These runs were initialised with the cell value set to the area-average rather than the cell-centre value. The differences are taken against an OpenFOAM reference solution with a resolution of 256×512 , coarser than the resolution of the spectral model (320×640) and so less accurate (in the tropics).

The errors are lower using the new cubic fit scheme. Importantly, the errors reduce when the mountain is refined whereas the errors actually increase when the mountain is refined using the quasi-cubic scheme. Also, oscillations occur at the mesh refinement boundary around the mountain when using the quasi-cubic scheme. For adiabatic, balanced cases such as this which are run for a long time, mesh refinement can actually degrade the errors globally if differencing schemes are used which give only first-order accuracy where the mesh is non-uniform. However, using the cubic fit scheme of [9] which gives higher-order accuracy where the mesh is non-uniform, mesh refinement on this case can lead to lower errors globally. This is crucially important if mesh refinement is to be used for weather or climate forecasting.

4. Conclusions

We have demonstrated that arbitrarily unstructured finite-volume modelling using OpenFOAM can compete with the accuracy of high-order structured techniques. A cubic differencing scheme has been implemented that maintains accuracy where the mesh is non-uniform. Hence 2:1 refinement of the mountain increases the accuracy globally. Using the previous quasi-cubic scheme, the order reduces to first where the mesh is not uniform and so 2:1 refinement patterns can actually make the global solution less accurate. This case is particularly sensitive to errors at refinement patterns because it is finely balanced, adiabatic and frictionless so any errors introduced in the long simulation persist and grow. A more complete model of the atmosphere will be sensitive in the same way but local refinement will offer more advantages where there are diabatic processes.

We have also demonstrated that a hexagonal-icosahedral mesh of the sphere gives accurate solutions since the mesh is nearly uniform globally. Unstructured meshes of polygonal shapes such as hexagons and pentagons could produce gradual local refinement although 2:1 refinement is more straightforward and efficient for high-order schemes.

Acknowledgements

We thank two anonymous reviewers for helpful comments, Nicholas Klingamann for improving the readability, John Thuburn for helpful discussions and Julia Slingso, NCAS and OpenCFD for support.

REFERENCES

1. A.S. Almgren, J.B. Bell, P. Colella, L.H. Howell, and M.L. Welcome. A conservative adaptive projection method for the variable density incompressible Navier-Stokes equations. *Journal of Computational Physics*, 142(1):1–46, 1998.
2. D.P. Bacon, N.N. Ahmad, T.J. Boybeyi, Z. and Dunn, M.S. Hall, P.C.S. Lee, R.A. Sarma, M.D. Turner, K.T. Waight, S.H. Young, and J.W. Zack. A dynamically adapting weather and dispersion model: The Operational Multiscale Environment Model with Grid Adaptivity (OMEGA). *Monthly Weather Review*, 128(7):2044–2076, 2000.
3. M.J. Berger and J. Olinger. Adaptive Mesh Refinement for Hyperbolic Partial Differential Equations. *Journal of Computational Physics*, 53:484–512, 1984.
4. G.S. Dietachmayer and K.K. Droegemeier. Application of continuous dynamic grid adaption techniques to meteorological modeling. part I: Basic formulation and accuracy. *Monthly Weather Review*, 120(8):1675–1706, 1992.
5. J.H. Ferziger and M. Perić. *Computational Methods for Fluid Dynamics*. Springer, 1996.
6. A. Iske and M. Kaser. Conservative semi-Lagrangian advection on adaptive unstructured meshes. *Numerical Methods for Partial Differential Equations*, 20(3):388–411, 2004.
7. C. Jablonowski, M. Herzog, J.E. Penner, R.C. Oehmke, Q.F. Stout, B. van Leer, and K.G. Powell. Block-structured adaptive grids on the sphere: Advection experiments. *Monthly Weather Review*, 134(12):3691–3713, 2006.
8. R. Jakob, J.J. Hack, and D.L. Williamson. Solutions to the shallow water test set using the spectral transform method. Technical note NCAR/TN-388+STR, Climate and Global Dynamics Division, National Center for Atmospheric Research, Boulder, Colorado, May 1993.
9. R.K. Lashley. *Automatic Generation of Accurate Advection Schemes on Structured Grids and their Application to Meteorological Problems*. PhD thesis, Departments of Mathematics and Meteorology, University of Reading, 2002.
10. M. Läufer, D. Handorf, N. Rakowsky, J. Behrens, S. Frickenhaus, M. Best, Dethloff K., and W. Hiller. A parallel adaptive barotropic model of the atmosphere. *Journal of Computational Physics*, 223(2):609–628, 2007.
11. W. Skamarock, J. Olinger, and R.L. Street. Adaptive grid refinement for numerical weather prediction. *Journal of Computational Physics*, 80(1):27–60, 1989.
12. R.K. Srivastava, D.S. McRae, and M.T. Odman. An adaptive grid algorithm for air-quality modeling. *Journal of Computational Physics*, 165(2):437–472, 2000.
13. A.N. Staniforth and H.L. Mitchell. Variable-resolution finite-element technique for regional forecasting with primitive equations. *Monthly Weather Review*, 106(4):439–447, 1978.
14. J. Thuburn. A PV-based shallow-water model on a hexagonal-icosahedral grid. *Monthly Weather Review*, 125(9):2328–2347, 1997.
15. J. Thuburn. Some conservation issues for the dynamical cores of NWP and climate models. *Journal of Computational Physics*, In press.
16. H.G. Weller, G. Tabor, H. Jasak, and C. Fureby. A tensorial approach to computational continuum mechanics using object-oriented techniques. *Computers in physics*, 12(6):620–631, 1998.
17. D.L. Williamson, J.B. Drake, J.J. Hack, R. Jakob, and P.N. Swartrauber. A standard test set for numerical approximations to the shallow water equations in spherical geometry. *Journal of Computational Physics*, 102:211–224, 1992.